On the dynamic monitoring of the variations in blood viscosity by resonant optical signal

L. Garnier[a], H. Lhermite[a], Timothée Labouret[b], A. St Jalmes[c], H. Cormerais[a,d], V. Vié[c], B. Bêche[*a]

[a]Université de Rennes, CNRS, Institut d'Électronique et des Technologies du numéRique - IETR UMR 6164 F-35000 Rennes, France; [b]SATT Ouest Valorisation, CS 80 804, F-35708 Rennes, France ; [c]Université de Rennes 1, CNRS, Institut de Physique de Rennes - IPR UMR 6251, F-35000 Rennes, France; [d]Centrale/Supelec, Campus de Rennes, F-35510 Cesson-Sévigné, France

*bruno.beche@univ-rennes1.fr; https://www.ietr.fr/bruno-beche

ABSTRACT

This study concerns the development of sensors based on integrated photonics and resonator elements for monitoring the dynamic processes of sedimentation and drying of various bloods. The resonant structures of integrated photonics were produced and shaped on Si/SiO_2 and organic UV210 substrate, by deposition and microlithography processes allowing achieving patterns of sub-wavelength dimensions. The micro-resonators produced could be incorporated into a detection platform and fine measurements thermally controlled, were performed thanks to a specific signal processing by implemented codes. The analyses and monitoring over time of the different bloods were carried out with an identical defined protocol. The different bloods studied were sampled respectively from poultry, goats and humans with various characteristics in terms of red blood cell sizes, viscosities and densities. The analyzes relating to the sedimentation rates, the viscosity measurements by rheometer and the images of the red blood cells were carried out by different methods and apparatus for all the blood studied. These latest corroborated by our specific resonant measurements on integrated chip and sensors allow us to converge and conclude that the device and photonic chip sensor produced can discriminate the different bloods, with in the 1st order, an equivalent and differential viscosity measurements. This work further proves that rheology by optical means (and not mechanically) is possible.

Keywords: Integrated photonics and resonators, optical characterizations, sensors, bloods, viscosity and rheology.

1. INTRODUCTION

In different industrial fields using so-called soft substances and matter[1,2] which present relatively slow dynamic variations[3], such as cosmetics with creams, oils and foams, food processing and milk industry with foams, pharmaceuticals with colloids and gels, energy with petroleum residues[4] (heavy fuel oil combustion control and contain impurities that can induce serious damages), organic micro-electronics with certain substances card development, medical with specific fluids, it is necessary to estimate relatively or more absolutely the property of viscosity[5]. Different types of rheometer and viscometer devices exist based on various architectures (tubular and capillary) and physical principles (vibrating/oscillating bodies, falling/rolling bodies, rotation)... As a known and school example based on Newton's second law and fundamental principle of mechanics, the falling ball viscometer which uses Stokes' law makes it possible to estimate the viscosity of fluids[6]. In this example, the architecture is in volume and requires a significant quantity of fluid to be studied, like all the currently existing techniques.

Moreover, in physics, many waves and oscillations can probe soft matter as a specific transfer function, such as mechanics of course, but also acoustics and optics waves. It should be noted that optics is particularly sensitive to visco-elasto-mechanics, compression/dilation, rigidity by laws of permittivity variations $\Delta\varepsilon$ (and therefore of index at optical frequencies), by variations in densities (macroscopic Gladstone law type). Finally the optical wave has different modulation mechanisms likely to imprint on its amplitudes (absorption), its phase, its coherence, its diffusion, its speckle, its fluorescence, its quality factor in term of resonance, the dynamic visco-mechanical variations of substances

crossed and probed. In this paper, we propose to study the dynamics of relative variation of the viscoelasticity of different blood substances by a resonant surface photonic signal probing this biological soft matter. In this study, we will realize ourselves the resonant elements specific to a micro-photonic[7,8] directly in contact with blood, then to its signal processing. Indeed, optical Micro-Resonators[9] (MRs) appears adequate to create such a resonant signal, because they are already used as sensors to detect various kind of substances for chemical, biological and medical applications[10-13]. Moreover last years, MRs have been also used to follow various dynamic transition process in soft matter (phase transitions, evaporations, loss of mass…)[14-16].

Regarding blood, these are plasmas and suspensions, complex with mixtures of species of different sizes and structures such as white blood cells (Leukocytes) and red blood cells (erythrocytes) plus protein macromolecules moving, coagulating, sedimenting at different velocities. By way of example, a simple blood volume sedimentation experiment makes it possible to visualize the hematocrit and therefore the volume of the red blood cells occupied in the complete blood. This complex biological plasma has also been probed by acoustic waves (ultrasound) in order to measure coagulation rates[17]. At the level of wave physics, blood over time must be seen as an evolving transfer function when it is probed by a wave with one or more frequency attributes. Thus, for optics, blood will constitute a medium that is certainly complex, but possesses optical[18] and physical properties of complex optical indices[19,20] (real/imaginary part and then transmission/absorption) of density which will moreover be linked to the macroscopic properties of such blood aspects such as its color, its ability to flow, to dry, its viscosity... At the microscopic level, the influence of the shape and size of the red blood cells, which are moreover intrinsically different depending on the animal[21], will induce such and such flow properties[22]. It should be noted that the physical properties of blood will by definition be liable to change during an infection or disease by excessive aggregation of red blood cells, increased sedimentation rates and other measurable phenomena[23].

Such paper is then devoted to the idea to track the dynamical viscoelasticity of various blood directly in contact to the optical surface resonant signal by following the associated consequences on the spectral characteristics of the resonant guided mode localized into the shaped organic MR. Such MR is characterized by its eigenvalue, namely the effective index of an optical mode propagating inside. According to the dispersion equation derived from the resolution of Maxwell equations, the effective index depends on the opto-geometrical features of the resonator, as well as its close viscoelastic environment. A progressive modification of the viscosity thus induces a temporal variation of the effective index that can be measured by the tracking of the Free Spectral Range (FSR) of the transduced spectra against time. To do so, racetrack shaped MRs are integrated on a chip by means of photolithography[24,25] and excited by a broadband laser. The transduced optical signal is then directed towards an Optical Spectrum Analyzer (OSA) from which spectra are acquired against time. The dynamic optical data collected by this way related to various king of blood are then compared to classical measurements of viscosity by a mechanic rheometer. The experimental setup, from the materials and fabrication of the photonic structure by photolithography, to the inclusion of this circuit in an optical characterization platform and the presentation of the data acquisition and treatment program are first described in section 2. Then, such experimental optical results based on the dynamic tracking of the resonant signal in contact with blood are analyzed and discussed in addition and parallel to being corroborated by mechanics rheometer measurements into the section 3.

2. MATERIALS, PROCESSES AND EXPERIMENTAL PLATEFORM

2.1 Design, fabrication procedures and materials

The design of the masks was established by software creating all the integrated photonic structures, namely, guides, tapers, resonators and so on. The 4 inch masks are then created on quartz/metal, the organic DUV 210[24,25] flashing at 248 nm. On a silicon substrate, a thermal silica layer is formed by wet oxidation method. We must first clean the wafer with the method RCA (developed by 'Radio Company of America'), to avoid all impurities. The plate is then put in a quartz oven with torch, the gas H2 and oxidation gas O_2 being located in the flame for the combustion. A typical 4h hours stage in the oven at 1175°C can form 1.6 µm of silica on the surface of the wafer, creating the silica lower cladding. After oxidation, the annealing at 700°C-800°C strengthens the single crystal structure. Such a thickness guarantees a highly stable and homogeneous refractive index under the organic waveguides and MRs so as to decrease the optical radiation losses regarding the propagation modes.

Figure 1 shows by way of example the type of structures drawn on software in the appropriate format plus an optical microscopy imaging (top view) of the structures produced. The resonator is laterally coupled to an access waveguide which features a taper structure that spatially compress the optical mode before it is coupled to the resonator. The presence of the taper structure facilitates the injection of light in the waveguide.

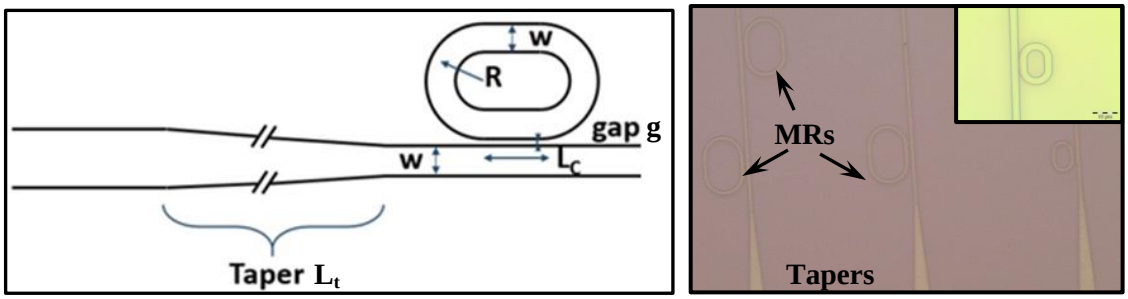

Figure 1. On the left, the schematic representation of the architecture of the resonant circuits used as sensors. A racetrack-shaped micro-resonator is coupled to an access waveguide and a taper structure (L_t) is present at the beginning of the latter in order to facilitate the injection by spatially compressing the guided mode. *R* represent the radius of curvature of the curved part of the resonator, L_c the coupling length between the resonator and the access waveguide, and *w* is the width of the waveguide. On the right, the optical microscopy imaging (top view) of the structures produced.

The circuits are fabricated in UV210, a polymer presenting an absorption band at 248 nm in the deep-UV domain, thus allowing to perform deep-UV photolithography. The deep-UV photolithography process at 248 nm allows the design of more precise and smaller structures compared to the traditional 'i-line' photolithography at 365 nm. The UV210 resin is spread on the surface of a thermally oxidized Si wafer by the means of the spin-coating technique. The photolithography process is then performed by means of a mask aligner (MJB4 Mask Aligner Suss MicroTec), a previously designed and fabricated mask (designed with Cadence Virtuoso software and fabricated by TOPPAN PHOTOMASK Inc.) as well as a mercury lamp (HBO 1000W/D, OSRAM) accompanied by the proper filter to select the $\lambda = 248$ nm wavelength. Once the illumination is performed, the circuits are developed by the use of tetra-methyl ammonium hydroxide (Microposit MF CD-26). The entire photolithography procedure is detailed on Table 1.

Table 1. Processes and parameters for the fabrication Si/SiO_2/UV210 photonic MRs and circuits.

Thermal oxidation (SiO_2 into Si)	**Parameters**
Humid pyrolitic oxidation (AET Technologies)	4h35min at 1175°C **- i)** O_2 (2 l/min) + N_2 (2 l/min) 5 min **- ii)** O_2 (2 l/min) 10 min **- iii)** H_2 (1.8 l/min) + O_2 (1 l/min) 4 h **- iv)** N_2 (2 l/min) 20 min
Photolithography procedure /steps (Organic UV210)	**Parameters**
Spin-coating (v,a,t), thickness, roughness	(900 rpm, 5000rpm/s, 30s), ~800-850 nm, <3 nm
Softbake	3 min at 140°C
Deep UV exposure + Post-exposure soft-bake	E = 20 mJ/cm² during 27 s + 1 min at 120°C
Development + Final softbake	30 s, with Microposit MF CD-26 + 24 h at 120°C

Once the circuits are integrated on the wafer, it is cleaved by the mean of a diamond tip to be incorporated in a test platform.

2.2 Optical platform and principles of measurements

Such Si/SiO_2/UV210 photonic structures and micro-resonators are based on a coupling and resonance physics, with a tunnel effect through a gap added with an optical geometric and cyclic resonance. The quantifications localize into the resonator emerge due to the installation of a cyclic condition (or stationary waves) written as $P_{opt} = t.\ \lambda$, with P_{opt} the 'optical'-perimeter of the micro-resonator, λ the optical wavelength of the light and *t* an integer. Quantifications can be measured by tracking the pseudo-period or Free Spectral Range (FSR) of the transduced spectra. Indeed, the FSR

verifies $FSR = \frac{\lambda_0^2}{\{P.n_{eff}^{gpe}\}} = \frac{\lambda_0^2}{\{P_{opt}\}}$, with λ_0 the central excitation wavelength and P the geometrical perimeter of the resonator. The resonator is excited by a broadband laser diode (SUPERLUM, SLD 331 HP3) with central wavelength $\lambda_0 = 795$ nm and $FWHM = 40$ nm. To do so, microscope objectives are used to inject the light in the photonic circuit and to defocalize the output signal. Then the transduced signal is directed to the Spectrum Analyzer Optical (OSA Ando AQ-6315E) or spectrometer (HR 4000, Ocean Optic) linked to a data acquisition and treatment program. A code in Matlab environment controls the spectrum analyzer and allows to record series of spectra successively while calculating the FSR. At each measurement experiment, a drop of blood (respectively goat, poultry, human) is deposited on the integrated chip by micro-pipette. The Figure 2 represents a photograph during an injection and tests with a drop of blood deposited.

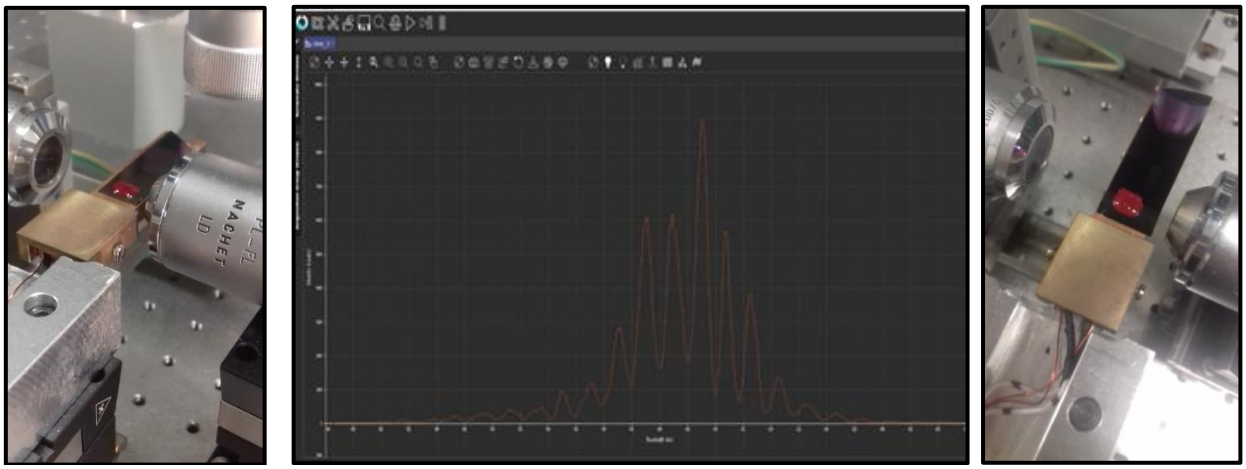

Figure 2. Optical photograph during an injection and tests with a 20 µl drop of blood deposited onto the MRs and chip. Middle, an example of a resonant spectral quantization from the surface photonic signal within an integrated resonator. The pseudo period of the spectrum corresponds to the FSR.

Blood containing red blood cells in suspension which sediment and aggregate by becoming denser above the resonators within a viscous plasma/fluid. Then, with a simplified view, the sedimentation[6] velocity can be obtained by applying the second Newton law on the equivalent spherical elements (red blood cells) considering its weight, the Archimede principle and the visquous friction force; such a procedure leads to an analytical expression of the sedimentation rate (Stokes law) : $v_{sed} = \frac{2}{9}\frac{gR^2(\rho_b - \rho_l)}{\eta}$. Furthermore, these sedimentation rate measurements have, already been demonstrated under a resonant light probe concerning nano-particles of variable sizes in water (η = 1mPa.s) and therefore 'non-viscous fluid'[26]. Now, parameters ρ_b and ρ_l represent the density of the spherical elements in suspension into a strong viscous plasma, and then R is the equivalent radius of the spherical elements as the red blood cells (erythrocytes), g the gravitational acceleration and η the dynamic viscosity of the fluid/plasma. It can be noted that the precedent model based on the Newton's second law is relevant for a single spherical particle, but does not take into account the collective effects, fragmented matter, such as the modification of the Einstein effective viscosity caused by the presence of multiple red blood cells suspension.

3. EXPERIMENTAL RESULTS, DISCUSSIONS AND CONCLUSION

3.1 Experimental measurements and results

All of the preceding parameters of Stokes' law (as rate sedimentation, radius R of red blood cells, viscosity η) are thus strongly linked into such one relation. In order to study and determine a possible mode of operation in an optical viscometer under surface resonant signal (on the FSR(t) measurement), we will have to decorrelate some of parameters by measuring them independently by so-called conventional and usual methods. Such will be the plan of experiment. First of all, the sedimentation rates were measured for each of the bloods by the Hematocrit technique in volume allowing in simple optical imaging to visualize over time the separation of the constituents from the top to the bottom that is plasma, then leukocytes and thrombocytes, then finally the erythrocytes (red blood cells) having

sedimented at the bottom of the tube. The measurements of the diameters of the red blood cells of each blood were obtained by a large number statistic of measurement from optical microscopic imaging. Then the viscosities measurements of each blood (overall blood and reb blood cells only) were performed with an Anton Paar (MCR 301) rheometer. The Figure 3 represents respectively these aspects, namely measurements of sedimentation rates by Hematocrit, imaging of red blood cells by optical microscopy and viscosities measurement.

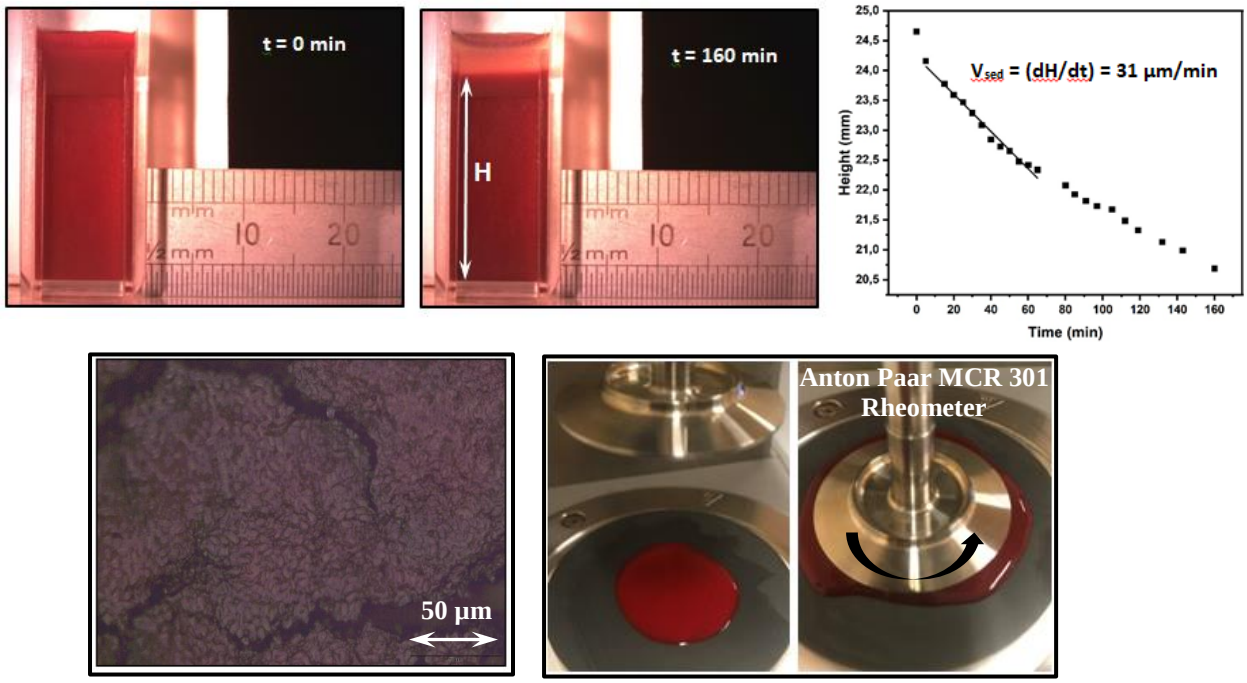

Figure 3. At the top, photographs and determination of the sedimentation rate by Hematocrit (Ht/HCT), case of poultry blood with v_{sed}= 31µm/min. Below, imagery by optical microscopy of red blood cells (erythrocytes), here the case of those of poultry blood and a diameter measurement statistic tending towards D=2R=3.95µm. Photographs of the rheometer (Anton Paar MCR 301) used to measure the viscosity η (mPa.s) of red blood cells from different blood types (poultry, goat, human). For this type of 'mechanical' rheology measurements typically 1 to 3 ml of red blood cells are minimum required.

Viscosity measurements by conventional mechanical or rheological method are typically carried out with 1 to 3 ml of blood spread under a fixed rotating part then at slow increasing speeds. In such configuration called 'cone-plane' geometry of the Anton Paar MCR 301 rheometer (its turning piece), such thickness presents a maximum of 0.9 mm at the maximum radius of 2.5 cm from the rotating part. Then, at a fixed rotational speed ω (rpm) of the rotating part, the advantage of the 'cone-plane' geometry is that the shear rate (velocity/thickness that is s^{-1} in unit) is uniform over the entire spread blood sample, indeed, when the radius of the rotating part increases, the speed of rotation also increases, but if the thickness also increases, then the shear rate remains constant over the whole of the puddle of blood spread. With such values of shear rate, the rotation of the piece is almost imperceptible at the beginning and at the end can reach 1 rpm, which is very slow.

Figure 4 on the left represents the viscosities values measured for different shear rates; the latter is expressed in s^{-1} being defined as the ratio of the velocity of displacement of the plate (see photography Figure 3) divided by the thickness of the fluid (blood). Note that poultry blood is the least viscous compared to goat and human blood. Moreover, it is the goat's blood which seems the most viscous, therefore sedimenting the slowest and also the densest, made up of the smallest red blood cells (diameter measured statistically at 2.05µm) and certainly tight in this overall blood and plasma.

One can imagine that the micro-structure of poultry and human blood made up of larger red blood cells (2 to 2.5 times) will allow easier rolling between them, this would explain in terms of image the viscosity measurements by the mechanical rheometer. It should also be noted that for each blood, the complete mixture of the only blood concerned with all its constituents (plasma, white and red blood cells, proteins) has always been measured more viscous than the red blood cell matter resulting from sedimentation or Hematocrit.

Then, as shown in Figure 2 that describes the chip sensor and principle of measurements onto the resonant signal, we thus recorded over time the variation of the pseudo-period (FSR) of the resonant surface signal. Figure 4 represents the evolution of this FSR parameter over measurement times of up to maximum 50 min. It is first of all possible to discriminate between the different bloods because the slopes of variation of the FSR are different. We have noticed that the evolution of the resonant signals (ΔFSR over time) of poultry is established much earlier than that of the very viscous goat blood.

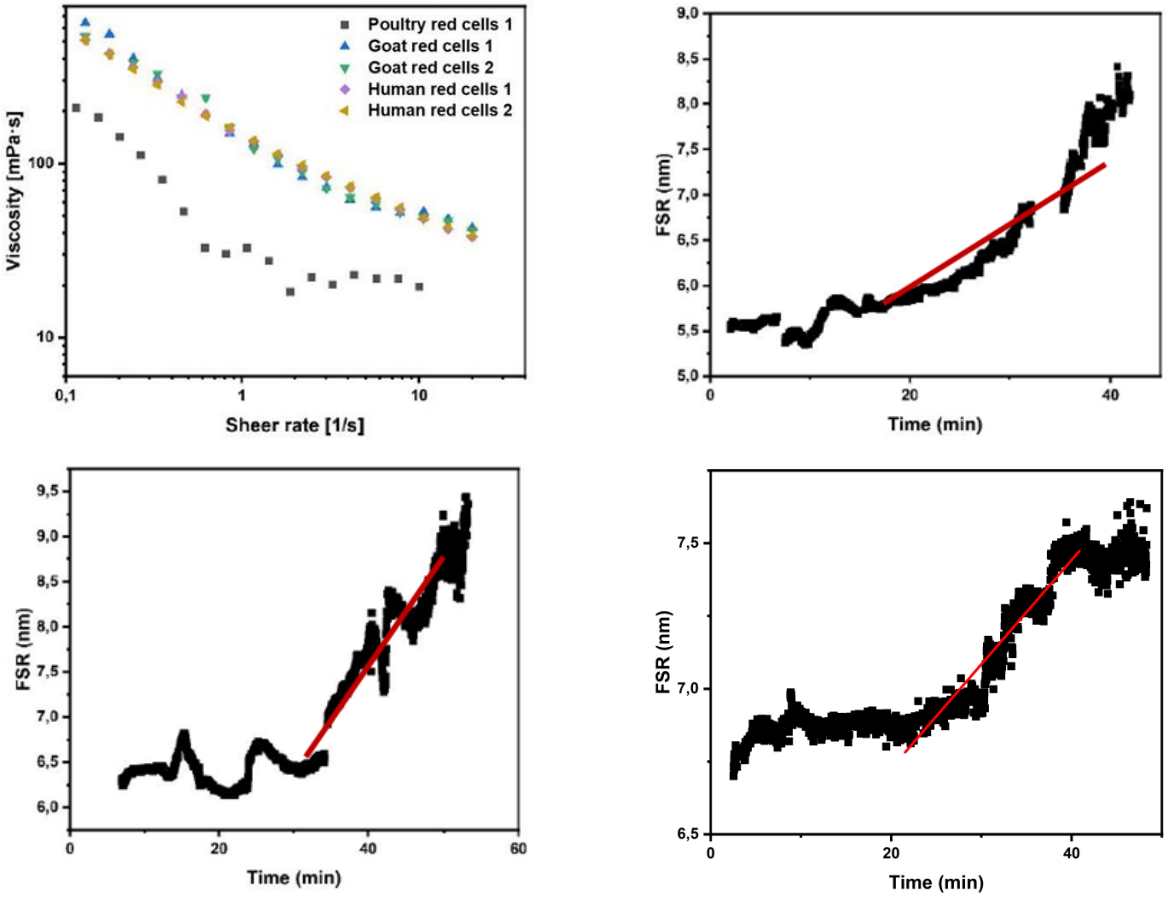

Figure 4. Comparison of viscosity η (mPa.s) measurements of different red blood cells (poultry, goat and human blood) by the rheometer (Anton Paar MCR 301); the number 1 and 2 on the same blood is only a double measurement in terms of statistics. For this type of 'mechanical' rheology measurements typically 1-3 ml of red blood cells are required. The resonant photonic measurements by the evolution of the FSR parameter respectively and as an example for the blood of poultry (high, right), goat (low, left) and human (low, right).

As the photonic measurements are made on an integrated circulating resonant light chip with only 20 µl of blood without rotation of the blood and just in sedimentation (densification plus 'compactus') of red blood cells, that causes an increase in material density Δρ (see Stokes law) of these above MRs, we considered the values of blood viscosities in quasi-static mode, namely the extra low shear rate of 0.1 s^{-1} so that it can be matched to an 'all-optical viscometer' possibility.

3.2 Discussions and conclusions

In such plan of experience, Table 2 represents all the values of the parameters measured (conventional methods plus the specific optical resonant method based on the pseudo-period FSR) so as to be able to analyze the effect and observe the links between parameters or between their relative ratios.

Table 2. All the parameters of Stokes' law and optical FSR respectively measured by usual techniques then by resonant photonic probe.

Bloods	**V_{sed} (µm/min)** (By volume measurements or Hematocrit)	**ΔFSR (nm/min)** (Measured by resonant surface wave sensor)	**η (mPa.s)** (Viscosity of red blood cells, shear 0.1 /s, measured by mechanical rheometer)	**D^2 (µm^2)** (Measured by optical imaging on average statistics)
Goat	4.4	0.090	680	$(2.05)^2$
Human	23.0	0.036	500	$(5.11)^2$
Poultry	31.0	0.045	205	$(3.95)^2$

During the sedimentation or densification Δρ of the blood, the so-called macroscopic law of Gladstone imposes a corresponding variation of the optical index $\Delta n \propto \Delta\rho$. Gladstone's law seems to have remained valid for all terrestrial materials and is expressed by the fact that (n-1)/ρ = cste. This is defined in optics by the fact that dense materials have higher optical indices (real index at wavelengths where they are transparent). With the resonant light configuration quantified by $FSR = \frac{\lambda_0^2}{P.n_{eff}^{gpe}}$ (with n_{eff} the eigenvalue of the resonant mode), a direct proportionality then follows between Δρ and the variation of the ΔFSR. Actually, $\Delta\rho \propto \Delta n \propto -\Delta FSR/(FSR)^2$, but we will consider for almost all the bloods that the FSR reference (at the start of the experiment and on a fixed MR's geometry), will be almost identical and therefore will be simplified in the following reasoning. For example, the FSR of the quantified optical signals is between 5.5, 6.25 and 6.75 nm at the start of the experiment for the three bloods studied.
It can be noted that the more compact the blood will be in the end, the greater the variation of the FSR should be on this model. This means that the Δρ (Gladstone law applied in optics) densification intervenes and will impact the result concerning the viscosity. Thus, by rewriting Stokes' law by this principle and Gladstone's law plus the correspondence in photonics between the variation of the density and that of the FSR, it is possible to form the ratio of Stokes' law for two different bloods.

Table 3. Comparison of relative parameter ratios for blood pairs (i, j indices represents two various and couples of bloods). $\Delta FSR_{i/j}$ in second line of the table represents the densification $\Delta\rho_{i/j}$ (Gladstone law and the resonant principle).

	Relative ratio of parameters (i/j)	**Goat/Poultry**	**Human/Poultry**	**Human/Goat**
Mechanics and Rheology	$\left[\frac{\eta_i}{\eta_j}\right]$	3.3	2.4	0.7
Optics and Resonance	$\frac{\left[\frac{(D_i)^2}{(D_j)^2}\right]}{\left[\frac{v_{sed.i}}{v_{sed.j}}\right]}\left[\frac{\Delta FSR_i}{\Delta FSR_j}\right]$	3.7	1.8	0.5

Such Table 3 presents the comparison between the relative ratio of the viscosities (measured by the mechanical rheometer, first line) and the equivalent of the viscosities obtained by a Stokes law translated and measured/felt by a quantified resonant light principle. We note a correspondence in terms of relative ratio, knowing that the use of Stokes' law is by definition a first simplification for a viscous and complex plasma/fluid filled with fragmented matter such as red blood cells. This also proves that the idea of using Gladstone's law integrated into this model (correspondence density, effective optical index in guidance, then FSR in resonance) has direct repercussions on the values of the FSR in resonant light configuration. Another simplification was made by not taking into account the values of the FSRs at the start of the experiment, and therefore by having considered them equal for all the bloods as mentioned previously. However, even if bloods are undoubtedly very complex biological fluids, all the correlations between the measurements viscosities, sedimentation rates, sizes of red blood cells and their possible rearrangement, then their increase of density close to the surface of the MRs seem to follow logical behaviors in terms of dynamics even with this simplified model.

Acknowledgments: The authors would like to thank the 'Société d'Accélération du Transfert de Technologies' (SATT Ouest Valorisation, Timothée Labouret also for our scientific discussions), the NanoRennes Plateforme (https://www.ietr.fr/plateforme-nr-nanorennes) for financially and help supporting this research. This study is also a part of a PASS_programm 'cordée de la réussite' named 'Pour une Ambition Scolaire Scientifique' (For a Scientific School Ambition) with the Brittany center (Sir Cyril Le-Corre and Madame Valérie Mesnet at Lycée Fulgence Bienvenüe, and Collèges Louis Guilloux, Paul Eluard, Romain Rolland, https://spm.univ-

rennes1.fr/les-cordees-de-la-reussite). The authors are very grateful to the people of INRAE for some blood samples, Mesdames Florence Gondret, Elodie Merlot, Eloise Delamaire, Nelly Muller, Gentlemen Philippe Lamberton, Josselin Delamare (INRAE) then Julien Recoquillay from Hubbard Breeders.

REFERENCES

[1] Brochard-Wyart, F., Nassoy, P. and Puech, P.H., [Physique de la matière molle], Dunod (2018).
[2] Cantat, I., Cohen-Addad, S., Elias, F., Graner, F., Hohler, R., Pitois, O., Rouyer, F. and St Jalmes, A., [Foams : structure and dynamics], Oxford University Press, (2013).
[3] Cipelletti, L. and Ramos, L., "Slow dynamics in glasses, gels and foams", Curr. Opin. Colloid Interface Sci. 12, 23-28 (2002).
[4] Guibet, J.C., "Caractéristiques des produits pétroliers ", Techniques de l'Ingénieur K325, 1-28 (1997).
[5] Le Neindre B., "Viscosité : Définitions et dispositifs de mesures", Techniques de l'Ingénieur K478, 1-12 (2004).
[6] Blazy, P., Jdid. E.A and Bersillon., J.L., "Décantation - Aspects théoriques", Techniques de l'Ingénieur J3450, 1-10 (1999).
[7] Adams, M.J., [Introduction to Optical Waveguides], John Wiley & Sons, New-York, (1981).
[8] Snyder, A.W. and Love, J.D., [Optical Waveguide Theory], 2d ed. Kluwer Academic Publishers, (2000).
[9] Rabus, D.G., [Integrated Ring Resonators: the Compendium], Springer-Verlag, New-York, (2007).
[10] Vollmer, F. and Arnold, S. "Whispering-gallery-mode biosensing: label-free detection down to single molecules", Nature Methods 5, 591-596 (2008).
[11] Chauvin, D., Bell, J., Leray, I., Ledoux-Rak, I. and Nguyen, C.T., "Label-free optifluidic sensor based on polymeric microresonator for the detection of cadmium ions in tap water", Sensors Actuators B 280, 77-85 (2019).
[12] Meziane, F., Raimbault, V., Hallil, H., Joly, S., Conédéra, V., Lachaud, J.L., Béchou, L., Rebière, D. and Dejous, C., "Study of a polymer optical microring resonator for hexavalent chromium sensing", Sensors Actuators B 209, 1049-1056 (2015).
[13] Castro Beltran, R., Huby, N., Vié, V., Lhermite, H., Camberlein, L., Gaviot, E. and Bêche, B., "A laterally coupled UV210 polymer racetrack micro-resonator for thermal tunability and glucose sensing capability", Adv. Dev. Mat. 1, 80-87 (2015).
[14] Li, Q., Vié, V., Lhermite, H., Gaviot, E., Moréac, A., Morineau, D., Bourlieu, C., Dupont, D., Beaufils, S. and Bêche, B., "Polymer resonators sensors for detection of sphingolipid gel/fluidphase transition and melting temperature measurement", Sensors Actuators Phys. A 263, 707-717 (2017).
[15] Castro Beltran, R. , Garnier, L., St Jalmes, A., Lhermite, H., Gicquel, E., Cormerais, H., Fameau, A.L. and Bêche, B., "Microphotonics for monitoring the supramolecular thermoresponsive behavior of fatty acid surfactant solutions", Opt. Comm. 468, 125773.1-7 (2020).
[16] Garnier, L., Lhermite, H., Vié, V., Pin, O., Liddel, Q., Cormerais, H., Gaviot, E. and Bêche, B., "Monitoring the evaporation of a sessile water droplet by means of integrated resonator", IoP J. Phys. D: Appl. Phys. 53, 125107.1-125107.10 (2020).
[17] Nam., K.H., Yeom, E., Ha, H. and Lee, J.J., "Simultaneous measurement of red blood cell aggregation and whole blood coagulation using high-frequency ultrasound", Ultrasound Med & Biol. 38, 468-475 (2012).
[18] Lindberg, L.G. and Öberg, P.A., "Optical properties of blood in motion", Optical Engineering 32, 253-257 (1993).
[19] Friebel, M. and Meike, M., "Determination of the complex refractive index of highly concentrated hemoglobin solutions using transmittance and reflectance measurements", J. Biomedical Optics 10, 064019.1-064019.5 (2005).
[20] Lazareva, E.K. and Tuchin, V.V., "Blood refractive index modelling in the visible and near infrared spectral regions", J. Biomedical Photonics & Eng. 4, 010503.1-010503.7 (2018).
[21] Bellier, S. and Cordonnier, N., "Les valeurs usuelles en hématologie vétérinaire", Revue Francophone des Laboratoires 420, 27-42 (2010).
[22] Enejder, A.M.K., Swartling, J., Aruna, P. and Anderson-Engels, S., "Influence of cell shape and aggregate formation on the optical properties of flowing whole blood", Appl. Opt. 42, 1384-1394 (2003).
[23] Yeom, E. and Lee, S.J., "Microfluidic-based speckle analysis for sensitive measurements of erythrocyte aggregation : A comparison of four methods for detection of elevated erythrocyte aggragation in diabetic rat blood", Biomicrofluidics 9, 024110.1-024110.15 (2015).
[24] Rohm and Haas Electronic Materials, "UV 210 Positive photoresist", April 2005, https://kayakuam.com/products/uv-210gs-positive-duv-photoresist/ (Kayaku Advanced Materials, Inc.'s, 2021).
[25] Duval, D., Lhermite, H., Godet, C., Huby, N. and Bêche, B. "Fabrication and optical characterization of sub-micronic waveguide structures on UV210 polymer", IoP J. Optics 12, 055501/1-055501/6 (2010).
[26] Garnier, L., Lhermite, H., Vié, V., Cormerais, H.. and Bêche, B. "Determination of Stokes velocitie and sedimentation rate by a photonic resonant signal", SPIE Int. Soc. Opt. Eng. , 11772 (117720L Optical Sensors), 1-7 (2021).